

# Phenomenology with unintegrated parton showers\*

Michal Deák

Instituto de Física Teórica UAM/CSIC, C/ Nicols Cabrera 13-15,  
Universidad Autónoma de Madrid, Cantoblanco, Madrid 28049, SPAIN

We introduce a backward evolution Monte Carlo algorithm implementation of the CCFM equation and present latest developments in phenomenology of hadron-hadron collisions for the Monte Carlo generator CASCADE.

## 1 Introduction

The BFKL and the CCFM equations offer possibility to formulate so called unintegrated parton density functions (uPDFs). In uPDFs, in contrast to parton density functions (PDFs), the dependence on the transversal momentum of parton  $\mathbf{k}$  is preserved. In PDFs, also sometimes called integrated parton density functions, the transversal momentum of the evolved parton density is integrated over, but on the other hand there is a dependence on a scale to which the PDF is evolved. The corresponding equation for evolution of PDFs is the DGLAP equation. Both uPDFs and PDFs depend on the longitudinal momentum fraction carried by the parton  $x$ . The latter gives us also a hint for relation between uPDFs -  $\mathcal{F}$  and PDFs -  $f$  which can be sketched by equation

$$xf(x, \mu) = \int_0^\mu d^2\mathbf{k} \mathcal{F}(x, \mathbf{k}) . \quad (1)$$

Equation (1) shows that  $\mathcal{F}(x, \mathbf{k})$  contains more information than the  $f(x, \mu)$ , one can therefore expect that uPDFs will be very interest for phenomenology. Note that the uPDFs obtained using the CCFM equation depend on the longitudinal momentum fraction  $x$ , the transversal momentum  $\mathbf{k}$  and a scale  $\mu$ . Indeed, particular studies [1–3] show that uPDFs, by looking on observables connected to transversal momentum of the final state particles, effectively contain information from higher orders of perturbation theory.

One of the most powerful methods, for solving evolution equations and obtain phenomenological results, is the probabilistic interpretation of their kernels and their implementation in Monte Carlo programs in a form of parton shower generators. In Monte Carlo programs every term in the expansion in  $\alpha_S$  of the solution of the evolution equation is interpreted as a chain of parton emissions. The solution is obtained by summing all relevant terms and integrating them over free kinematic variables. In the previous paragraph we mentioned two different approaches to partonic content of the proton. From the point of view of a parton shower generator the difference is not so obvious. In a Monte Carlo program, which is solving the DGLAP equation

---

\*Preprint number: IFT-UAM/CSIC-11-21

and using PDFs as an initial condition, the transversal momentum of the last parton in the chain can be left free from integration and one can effectively obtain an uPDF which will also depend on the scale  $\mu$  (situation is similar to the one for the CCFM uPDFs). Most of the differences between the approaches with PDFs and uPDFs is in the dynamics, small  $x$  resummation in the BFKL and the CCFM equations, but also in the way how is the transversal reflected in the kinematics of the parton. In the BFKL and the CCFM equation the partons are off-shell by  $k^2 = -\mathbf{k}^2$ . In the DGLAP approach partons are kept on-shell which requires reshuffling of components of momenta [4].

It seems that the truly unintegrated approach is more consistent and offers also richer dynamics. We will describe theoretical foundations and phenomenological results Monte Carlo generator CASCADE [5] based on the CCFM equation.

## 2 The CCFM equation for a Monte Carlo generator

In the limit when the longitudinal proton momentum fraction  $x$  carried by the parton is very small,  $x \ll 1$ , the proton structure is dominated by the gluon component. The leading order in the BFKL equation includes only gluons. The CCFM equation can be formulated for the gluon uPDF, just by extending the BFKL equation by  $1/(1-z)$  term in the splitting function and angular ordering of gluon emissions. There is also a formulation of the CCFM equation for the valence quark uPDF which we will return to later.

The probability density for a splitting of a gluon into two gluons with angular ordering constraint will be (without inclusion of small- $x$  virtual corrections)

$$d\mathcal{P}_i^\theta = \frac{\alpha_S}{2\pi} dz_i \frac{d^2 \mathbf{q}'_i}{\mathbf{q}'_i{}^2} \hat{P}_{gg}(z_i) \Theta(|\mathbf{q}'_i| > z_{i-1} |\mathbf{q}'_{i-1}|) \Theta(1 - z_i - \epsilon) \quad (2)$$

with the first  $\Theta$ -function forcing angular ordering and the second introducing an infrared regulator  $\epsilon$ , which can be shown has to be  $\epsilon = \frac{Q_0}{|\mathbf{q}'_i|}$  [6], with  $Q_0$  being a constant infrared cut-off. Variable  $\mathbf{q}'_i = \mathbf{q}_i/(1-z_i)$  is introduced as the transverse momentum of the emitted parton rescaled by factor  $1/(1-z_i)$ . By  $\hat{P}_{gg}(z)$  we denote the gluon to gluon splitting function devoid of its non-singular terms.

Virtual corrections have to be included also into the splitting function used in the CCFM equation. The difference between the virtual correction factors of the BFKL and the DGLAP is that to be consistent one should apply the angular ordering condition also for the virtual corrections included in them.

The Sudakov form factor will read

$$\Delta_S(\mathbf{q}'_i{}^2, (z_{i-1} \mathbf{q}'_{i-1})^2) = \exp \left( - \int_{(z_{i-1} \mathbf{q}'_{i-1})^2}^{\mathbf{q}'_i{}^2} \frac{d^2 \mathbf{q}'}{\mathbf{q}'^2} \int_0^{1-\frac{Q_0}{|\mathbf{q}'|}} dz \frac{\alpha_S}{\pi} \frac{N_C}{1-z} \right). \quad (3)$$

The Non-Sudakov form factor is

$$\Delta_{NS}(\mathbf{k}_i{}^2, (z_{i-1} \mathbf{q}'_{i-1})^2) = \exp \left( - \int_{(z_{i-1} \mathbf{q}'_{i-1})^2}^{\mathbf{k}_i{}^2} \frac{d\mathbf{q}^2}{\mathbf{q}^2} \int_{z_i}^1 dz \frac{\alpha_S}{\pi} \frac{N_C}{z} \right) \quad (4)$$

in analogy to Regge form factor used in the BFKL equation respectively. The CCFM equation reads

$$\mathcal{F}(x, \mathbf{k}, \mathbf{q}'^2) = \mathcal{F}(x, \mathbf{k}, \mathbf{q}_0'^2) + \int_{\mathbf{q}_0'^2}^{\mathbf{q}'^2} \frac{d^2 \bar{\mathbf{q}}'}{\bar{\mathbf{q}}'^2} \frac{N_C \alpha_S}{\pi} \int_x^{1-\frac{Q_0}{|\bar{\mathbf{q}}'|}} \frac{dz}{z} \mathcal{F}(x/z, \mathbf{k}', \bar{\mathbf{q}}'^2) \left( \frac{\Delta_{NS}(\mathbf{k}'^2, (z\bar{\mathbf{q}}')^2)}{z} + \frac{1}{1-z} \right) \Delta_S(\mathbf{q}_0'^2, (z\bar{\mathbf{q}}')^2), \quad (5)$$

where  $\mathbf{k}' = \mathbf{k} + \mathbf{q}$ . The presence of the term responsible for soft gluon emissions in the CCFM splitting function provides summation of logarithms of  $\mathbf{q}'^2/\mathbf{q}_0'^2$  in addition to the  $1/x$  logarithms summed by the BFKL equation in leading logarithmic precision.

The Sudakov form factor (3), which gives the probability of no emission between to values of the evolution scale, is used to determine the value of the evolution scale for the next emission.

Appearance of the Non-Sudakov form factor (4) and gluon virtuality brings technical difficulties in backward evolution formulation of the parton shower. A solution is presented in [5].

### 3 Fits of uPDFs

In [7] this parameterisation was used to fit initial CCFM gluon uPDF at the starting scale  $Q_0 = 1.2 \text{ GeV}$

$$xA_0(x, k_t) = Nx^{-B}(1-x)^C(1-Dx)e^{-(k_t-\mu)^2/\sigma^2} \quad (6)$$

where  $N, B, C, D, \mu, \sigma$  should be in principle determined from fits. In practice, for the purpose of the study some parameters were fixed to  $C = 4$ ,  $\mu = 0 \text{ GeV}$ ,  $\sigma = 1 \text{ GeV}$  [8]. The value of parameter  $C$  is dictated by the spectator counting rules [9]. Fit of  $\chi^2/\text{n.d.f.} = 1.4$  was achieved.

Authors of [7] used a grid in the parameter space to parameterise the  $ep$  cross section obtained from the CASCADE Monte Carlo generator and to fit the  $ep$  cross section obtained from HERA data. Details of the technique can be found in the publication.

## 4 Forward jets in Monte Carlo generators PYTHIA and CASCADE

The analytical results for forward jet production which are implemented in Monte Carlo generator CASCADE can be found in [1]. More complete discussion of numerical results is available in [10].

### 4.1 Transverse momentum spectra

In Fig. 1 the prediction of differential cross section  $\frac{d\sigma}{dp_\perp}$  is shown as obtained from CASCADE and PYTHIA. The cross sections predicted from both simulations at low momentum are of the similar order, however, at larger transverse momentum the CASCADE predicts a larger cross section what is clearly visible for central jets (Fig. 1 right). This behavior is expected since CASCADE uses matrix elements which are calculated within high energy factorization scheme

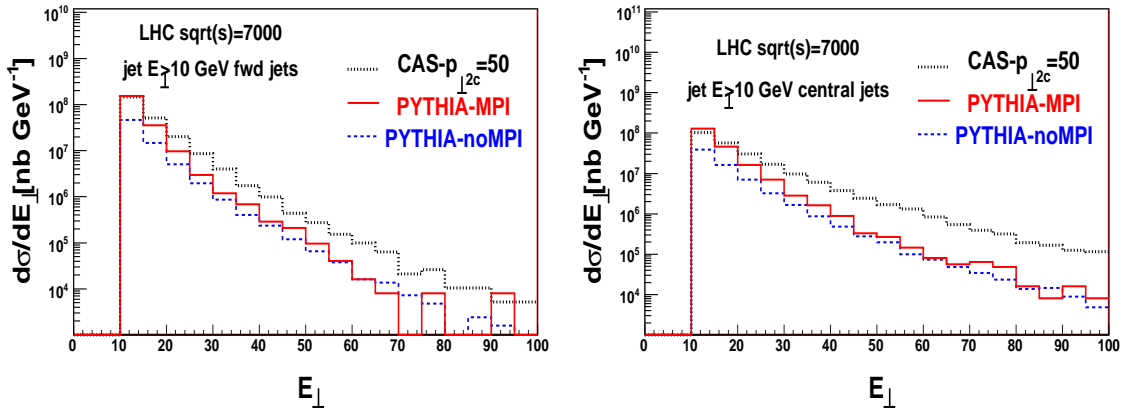


Figure 1: *Transversal momentum spectra of produced jets at total collision energy  $\sqrt{s} = 7\text{ TeV}$  with requirement that  $p_{\perp} > 10\text{ GeV}$ . We compare predictions obtained from CASCADE and PYTHIA running in a multiple interactions mode and no multiple interactions mode. Spectrum of forward jets (left); spectrum of central jets (right).*

allowing for harder transversal momentum dependence as compared to collinear factorization. Moreover CASCADE applies CCFM parton shower utilizing angle dependent evolution kernel which at small  $x$  does not lead to ordering in transverse momentum, and thus allow for more hard radiations during evolution as compared to based on leading order DGLAP splitting functions Monte Carlo generator PYTHIA. The parton shower has major influence on the side where the small  $x$  gluon enters the hard interaction, thus the jets in the central region are mainly affected by the parton shower.

## 4.2 Rapidity dependence

In fig. 2 we show prediction for pseudorapidity dependence of the cross section in two regions  $0 < |\eta| < 2$  and  $3 < |\eta| < 5$ . We see that results from CASCADE interpolate between PYTHIA with multiple interactions in the central region and PYTHIA without multiple interactions in the forward region. The result is due to the fact that CASCADE (because of angular ordering), and PYTHIA with multiple interactions (because of multi chain exchanges), predict more hadronic activity in the central rapidity region as compared to the collinear shower. In the remaining rapidity region cascade uses collinear parton shower of a similar type as in PYTHIA without multiple interactions.

## 5 $ZQ\bar{Q}$ production in MCFM and CASCADE Monte Carlo generators

To compare with a collinear NLO calculation, we use again the Monte Carlo generator MCFM. This Monte Carlo generator provides the process  $gg \rightarrow Zb\bar{b}$  at NLO only in the massless quark limit. To avoid divergences, additional cuts are applied on transversal momenta of quarks, on

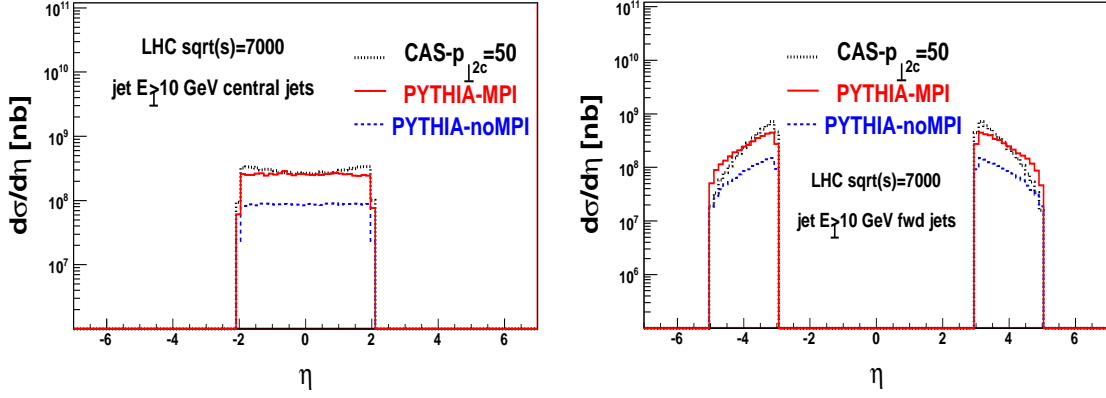


Figure 2: Pseudorapidity spectra of produced jets at total collision energy  $\sqrt{s} = 7 \text{ TeV}$  with requirement that  $p_T > 10 \text{ GeV}$ . We compare predictions obtained from CASCADE and PYTHIA running in multiple interactions mode and no multiple interactions mode. Spectrum of forward jets (left); spectrum of central jets (right).

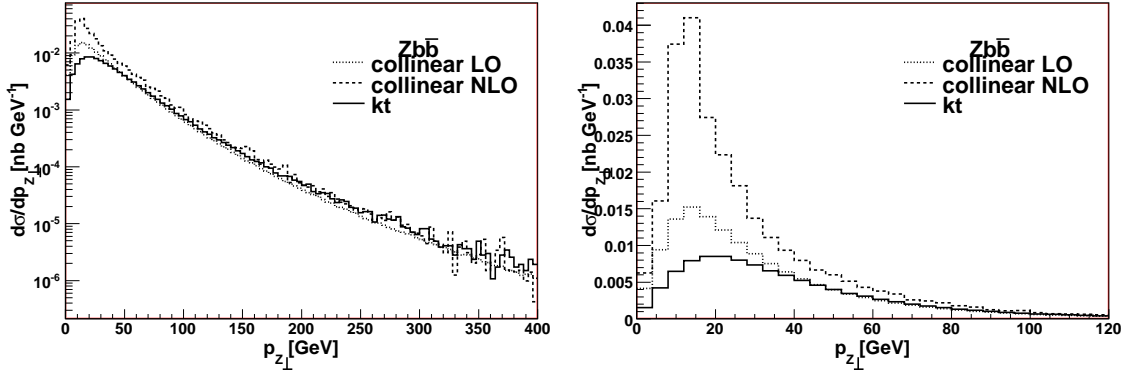


Figure 3: Transversal momentum spectrum of the Z boson produced associated with a  $b\bar{b}$  pair. Plotted in logarithmic scale (left) and in linear scale (right).

the invariant mass of the  $b\bar{b}$  pair, and on transversal momenta of a gluon which is produced in diagrams of real NLO corrections. Transversal momenta of produced quark, antiquark and gluon have to satisfy the condition  $p_{\perp} > 4.62 \text{ GeV}$  (corresponding to the mass of the  $b$ -quark). These cuts on quark (antiquark) momenta are automatically applied in MCFM when one is performing a calculation involving massless quarks (antiquarks). We choose the parton density functions set CTEQ6M [11]. The same cuts on transversal momenta of quark and antiquark are then applied in CASCADE as well.

The result for the cross sections differential in the transversal momentum of  $Z$  can be seen in Fig. 3 left. The cross section changes especially at small  $p_{Z\perp}$  (see Fig. 3 right) from LO to NLO calculation, and the difference between collinear calculation and  $k_T$ -factorization calculation becomes more pronounced. We observe that the maximum of the distribution in the NLO calculation (MCFM) stays approximately at same value of transversal momenta and the shape of the peak is very different from the one we obtain in  $k_T$ -factorization. Nevertheless, the  $p_{Z\perp}$  distributions match at very high  $p_{Z\perp}$  ( $\mathcal{O}(10^2\text{GeV})$ ).

The broadening of the peak by inclusion of small  $x$  effects which can be seen in Fig. 3 is consistent with prediction of [12].

## 6 Acknowledgments

I want to thank Alessandro Bachetta, Hannes Jung, Francesco Hautmann, Albert Knutsson, Krzysztof Kutak and Federico von Samson-Himmelstjerna for having the pleasure to include results of their work in my presentation at XL ISMD 2010 in Antwerp, Belgium.

## References

- [1] M. Deak, F. Hautmann, H. Jung, and K. Kutak, *JHEP* **09**, 121 (2009). 0908.0538.
- [2] M. Deak and F. Schwennsen, *JHEP* **09**, 035 (2008). 0805.3763.
- [3] S. P. Baranov, A. V. Lipatov, and N. P. Zotov, *Phys. Rev.* **D77**, 074024 (2008). 0708.3560.
- [4] Z. Nagy and D. E. Soper, *JHEP* **09**, 114 (2007). 0706.0017.
- [5] H. Jung and G. P. Salam, *Eur. Phys. J.* **C19**, 351 (2001). hep-ph/0012143.
- [6] G. Marchesini and B. R. Webber, *Nucl. Phys.* **B310**, 461 (1988).
- [7] A. Bacchetta, H. Jung, A. Knutsson, K. Kutak, and F. von Samson-Himmelstjerna (2010). hep-ph/1001.4675.
- [8] H. Jung, *Comput. Phys. Commun.* **143**, 100 (2002). hep-ph/0109102.
- [9] S. J. Brodsky and G. R. Farrar, *Phys. Rev. Lett.* **31**, 1153 (1973).
- [10] M. Deak, F. Hautmann, H. Jung, and K. Kutak (2010). 1012.6037.
- [11] J. Pumplin, D. Stump, J. Huston, H. Lai, P. Nadolsky, and W. Tung, *JHEP* **0207**, 012 (2002).
- [12] S. Berge, P. M. Nadolsky, F. Olness, and C. P. Yuan, *Phys. Rev.* **D72**, 033015 (2005). hep-ph/0410375.